Highlights

Regulating neuronal excitation or inhibition via magnetic field coupling

Zhenghui Wen, Chunhua Wang, Quanli Deng, Hairong Lin

- The ion exchange in neurons can trigger time-varying magnetic fields that interact with each other
- Magnetic field coupling can be considered as a way to modulate the neuronal excitation
- When the inhibition magnetic field coupling is large enough, the neuronal firing mode is static
- the magnetic coupling and synaptic coupling equations are compared

Regulating neuronal excitation or inhibition via magnetic field coupling

Zhenghui Wen, Chunhua Wang*, Quanli Deng, Hairong Lin

College of computer science and electronic engineering, Hunan University, Changsha, 410082, China

Abstract

The ion exchange in neurons can trigger time-varying magnetic fields that interact with each other. In this work, the regulation of neuronal excitation and inhibition by coupling magnetic field is investigated. Firstly, models of magnetic field coupling under different conditions are proposed. The effect of the magnetic field is described by magnetic flux. And then, the excitation or inhibition magnetic field coupling is studied under different external excitation currents. The firing mode of neurons can be changed by adjusting the coupling intensity. In brief, we found that the magnetic field coupling can regulate the excitation and inhibition of neurons, and the excitation magnetic field coupling can promote the firing of neurons. When the inhibition magnetic field coupling is large enough, the neuronal firing mode is static. Magnetic field coupling can be considered as a way to modulate the neuronal excitation. In the end, the magnetic coupling and synaptic coupling equations are compared and the effects of modulation of magnetic field coupling on neuronal excitation and inhibition are investigated. Studying the magnetic field coupling of neurons is important for understanding how neurons transmit information.

Keywords: magnetic field coupling, Electromagnetic induction, Inhibition and excitation, Hindmarsh–Rose neuron
PACS: 0000, 1111
2000 MSC: 0000, 1111

*Corresponding author
Email address: wch1227164@hnu.edu.cn (Chunhua Wang)

1. Introduction

The membrane potential of a neuron is the difference in the concentration of charged ions inside and outside the membrane. When a neuron transmits information, charged ions move in and out of the cell membrane to generate an action potential. According to the Maxwell electromagnetic induction theorem, the movement of charged ions can trigger time-varying electromagnetic fields. The impact of magnetic fields on information transmission to neurons can help us better understand and explore life's mysteries.

The memristor is the fourth basic circuit element, representing the mathematical relationship between charge and flux [1]. Coexistence attractor [2–4], hidden attractor [5–7], hyperchaotic attractor [8–10], circular chaotic attractors[11] and other phenomena have been identified in the research of chaos based on memristor, and such complicated dynamics have been exploited to encrypt [12–14]. Memristors have been used in circuit elements to simulate biological synaptic functions [15–17]. Various types of memristors were also being proposed. Fractional-order memristor[18–20], local active memristor [21–23], and so on.

Inspired by the magnetic flux physical characteristics of memristor [1], Ma et al. proposed to introduce magnetic flux into neuron model and HR neuron model under electromagnetic radiation in 2016 to obtain a variety of discharge modes [24, 25]. Based on this theory, The dynamic behaviors of different neuron models under electromagnetic radiation were explored [26–29]. For example, under the stimulation of electromagnetic radiation, FHN neurons can produce hidden extreme multistability phenomena [26]. Complex hidden cluster discharge patterns can be formed when the electromagnetic induction effect was applied to HR neurons[27]. The electrical activities of neurons under the electric fields were also considered in Refs. [28, 29]. Introducing external electromagnetic radiation through an inductor coil, Ref.[30] proposed a new neuron model under the influence of time-varying electric and magnetic fields as well as external electromagnetic radiation. By introducing Hamiltonian energy to measure magnetic field energy, the relationship between different neuron discharge modes and energy under electromagnetic radiation were studied, such as HR neuron [31, 32], FHN neuron [33, 34], and Izhikevich neuron[35, 36]. The researchers looked beyond the effects of electromagnetic radiation on neurons to neural networks. In Refs [37, 38], the chaotic dynamic behavior of the Hopfield neural network under the influence of external electromagnetic radiation on some neurons has been studied. The

influence of different external stimuli on the chaotic dynamics of the Hopfield neural network was studied, and the energy transfer phenomenon of the neural network under different stimuli was studied from the perspective of Hamiltonian energy[39]. The modulation of different kinds of external electromagnetic stimulation on the dynamics of the Newman-Watts small-world neural network model proved the feasibility of external electromagnetic stimulation to control the evolution of the neural network model [40].

Neurons send messages to each other through synapses that can excite or inhibit them. It would be interesting to discover another efficient method of signaling communication between neurons. In [41], scholars studied magnetic field coupling, which was the interaction between neuron magnetic fields, and proposed the coupling neuron model. When both magnetic field coupling and electrical synaptic coupling exist in neural networks, magnetic field coupling can regulate the collective behavior of neural networks [42, 43]. In the case, that magnetic field coupling, electric field coupling and synaptic coupling simultaneously act on the Newman-Watts small-world neuronal network, standard deviation and synchronization factor are introduced to provide useful guidance for signal transmission between neurons [44]. The above studies suggest that magnetic field coupling is another way of neuron signal propagation.

However, it is a pity that the excitability and inhibition of neurons regulated by magnetic field coupling are seldom considered in previous work. Synapses can make neurons excited or inhibited. As magnetic field coupling is another way of neuron signal communication, the regulation of magnetic field coupling on neuron excitation or inhibition should also be considered.

Based on the above discussion, this paper puts forward the concept of excitation and inhibition of magnetic field coupling and proposes the corresponding theoretical model. According to Abe's theorem, the direction of the magnetic field is determined by the direction of ion movement. Therefore, the excitation and inhibition of neurons can be indicated by the direction of the magnetic field. Based on this principle, the excitatory magnetic field coupling and inhibitory magnetic field coupling models are proposed. It is verified that excitatory magnetic field coupling can promote neuron excitation, inhibitory magnetic field coupling can inhibit the corresponding neuron, and the increase of coupling intensity to a certain degree makes the neuron reach the static state.

The following of this paper is organized as, section 2 presents a model for connecting two neurons with different types of magnetic fields; Section

3 studies two magnetic field coupling states under four discharge modes; Section 4 summarizes the full text.

2. Model description and scheme Considered

Synapses are the connections between neurons. And the importance of magnetic coupling as a possible way of transmitting information between neurons is undeniable. In order to study the modulation of excitation or inhibition of coupling neurons by magnetic field coupling. In this paper, we consider the response of the magnetic field coupled HR model to external stimulus currents in two cases: Case I. Excitatory magnetic field coupling model; Case II. Inhibitory magnetic field coupling model.

2.1. Excitatory magnetic field coupling model

In [41], a model of interaction between neuron magnetic fields was presented. In Refs [42, 44, 45], electrical synapses and magnetic fields were used for information interaction between neurons. and the two neurons connected by electrical synapses were both excited, so it can be considered that the magnetic coupling connecting the two excited neurons is also excitatory magnetic coupling. The corresponding excitatory magnetic field coupling model is shown below:

$$\begin{cases} \dot{x}_1 = y_1 - a{x_1}^3 + b{x_1}^2 - z_1 + I_{ext} - k\rho(\varphi_1)x_1 \\ \dot{y}_1 = c - d{x_1}^2 - y_1 \\ \dot{z}_1 = r[s(x_1 + 1.6) - z_1] \\ \dot{\varphi}_1 = k_1 x_1 - k_2\varphi_1 + G_{ex}(\varphi_2 - \varphi_1) \\ \dot{x}_2 = y_2 - a{x_2}^3 + b{x_2}^2 - z_2 + I_{ext} - k\rho(\varphi_2)x_2 \\ \dot{y}_2 = c - d{x_2}^2 - y_2 \\ \dot{z}_2 = r[s(x_2 + 1.6) - z_2] \\ \dot{\varphi}_2 = k_1 x_2 - k_2\varphi_2 + G_{ex}(\varphi_1 - \varphi_2), \end{cases} \tag{1}$$

where x, y, z and φ describe the membrane potential, recovery variables of slow current and adaptive current, and magnetic flux respectively. I_{ext} is the external stimulus current, the memristor coupling magnetic flux and membrane potential, its conductivity is $\rho(\varphi) = \alpha + 3\beta\varphi^2$. $G_{ex}(\varphi_1 - \varphi_2)\text{and}G_{ex}(\varphi_2 - \varphi_1)$, which represents the interaction of two magnetic fields. G_{ex} represents the coupling strength of the corresponding excitatory magnetic field, and the other parameters (a, b, c, d, k, r, s, k1, k2) are constants as (1.0, 3.0, 1.0, 5.0, 1, 0.006, 4, 0.5, 0.5).

2.2. Inhibitory magnetic field coupling model

It is well known that synapses can be divided into inhibitory and excitatory synapses. Inhibitory synapses connect the neurons, and the presynaptic neuron is activated while the postsynaptic neuron is inhibited. In this paper, magnetic field coupling is another way of neuron information transmission. Therefore, there is also a corresponding inhibitory magnetic field coupling. That is, the upper-level neuron is activated, while the lower-level neuron is inhibited, and they communicate with one another via magnetic field coupling. In this work, we propose the inhibitory magnetic field coupled two neuron model as:

$$\begin{cases} \dot{x}_1 = y_1 - a{x_1}^3 + b{x_1}^2 - z_1 + I_{ext} - k\rho(\varphi_1)x_1 \\ \dot{y}_1 = c - d{x_1}^2 - y_1 \\ \dot{z}_1 = r[s(x_1 + 1.6) - z_1] \\ \dot{\varphi}_1 = k_1 x_1 - k_2\varphi_1 - G_{in}(\varphi_2 + \varphi_1) \\ \dot{x}_2 = y_2 - a{x_2}^3 + b{x_2}^2 - z_2 + I_{ext} - k\rho(\varphi_2)x_2 \\ \dot{y}_2 = c - d{x_2}^2 - y_2 \\ \dot{z}_2 = r[s(x_2 + 1.6) - z_2] \\ \dot{\varphi}_2 = k_1 x_2 - k_2\varphi_2 + G_{in}(\varphi_1 + \varphi_2), \end{cases} \tag{2}$$

where Gin is the coupling strength of the corresponding inhibitory magnetic field. It is well known that adjusting the applied excitation current can alter the firing pattern of neurons. In order to explore the influence of different degrees of magnetic field coupling intensity on neuronal firing mode under different circumstances, we studied two magnetic field coupling cases of the proposed model with four different firing patterns, as shown in Table 1.

Table 1: cases of different firing states according to magnetic field coupling types

Different states	$I_{ext} = 1.8$	$I_{ext} = 2.3$	$I_{ext} = 3.2$	$I_{ext} = 4$
Excited-Excited	Sec3.1-Case1	Sec3.1-Case2	Sec3.1-Case3	Sec3.1-Case4
Excited-Inhibited	Sec3.2-Case1	Sec3.2-Case2	Sec3.2-Case3	Sec3.2-Case4

2.3. Stability analysis for the equilibrium states

The equilibrium Eq. (3) is found by zeroing the left side of Eq. (1)

$$\begin{cases} y_1 - a{x_1}^3 + b{x_1}^2 - z_1 + I_{ext} - k\rho(\varphi_1)x_1 = 0 \\ c - d{x_1}^2 - y_1 = 0 \\ r[s(x_1 + 1.6) - z_1] = 0 \\ k_1 x_1 - k_2\varphi_1 + G_{ex}(\varphi_2 - \varphi_1) = 0 \\ y_2 - a{x_2}^3 + b{x_2}^2 - z_2 + I_{ext} - k\rho(\varphi_2)x_2 = 0 \\ c - d{x_2}^2 - y_2 = 0 \\ r[s(x_2 + 1.6) - z_2] = 0 \\ k_1 x_2 - k_2\varphi_2 + G_{ex}(\varphi_1 - \varphi_2) = 0, \end{cases} \tag{3}$$

The equations may be solved using MATLAB, and the real solution is the equilibrium point. The following approach is used to construct the Jacobian matrix corresponding to Eq. (1).

$$J = \begin{pmatrix} J_{11} & 1 & -1 & J_{14} & 0 & 0 & 0 & 0 \\ J_{21} & -1 & 0 & 0 & 0 & 0 & 0 & 0 \\ J_{31} & 0 & J_{33} & 0 & 0 & 0 & 0 & 0 \\ J_{41} & 0 & 0 & J_{44} & 0 & 0 & 0 & J_{48} \\ 0 & 0 & 0 & 0 & J_{55} & 1 & -1 & J_{58} \\ 0 & 0 & 0 & 0 & J_{65} & -1 & 0 & 0 \\ 0 & 0 & 0 & 0 & J_{75} & 0 & J_{77} & 0 \\ 0 & 0 & 0 & J_{84} & J_{85} & 0 & 0 & J_{88} \end{pmatrix} \tag{4}$$

where $J_{11} = 2bx_1 - 3ax_1^2 - k(\alpha + 3\beta\varphi_1^2)$; $J_{21} = -2dx_1$; $J_{31} = J_{75} = rs$; $J_{85} = J_{41} = k_1$; $J_{14} = -6k\beta\varphi_1 x_1$; $J_{33} = J_{77} = -r$; $J_{88} = J_{44} = -k_2 - G_{ex}$; $J_{48} = J_{84} = G_{ex}$; $J_{55} = 2bx_2 - 3ax_2^2 - k(\alpha + 3\beta\varphi_2^2)$; $J_{65} = -2dx_2$; $J_{58} = -6k\beta\varphi_2 x_2$.

The eigenvalues of the appropriate equilibrium point are calculated by substituting it into the Jacobian matrix. Table 2 summarizes the findings.

The related equilibrium Eq. (5) is found by zeroing the left side of Eq. (2).

$$\begin{cases} y_1 - a{x_1}^3 + b{x_1}^2 - z_1 + I_{ext} - k\rho(\varphi_1)x_1 = 0 \\ c - d{x_1}^2 - y_1 = 0 \\ r[s(x_1 + 1.6) - z_1] = 0 \\ k_1 x_1 - k_2\varphi_1 - G_{in}(\varphi_2 + \varphi_1) = 0 \\ y_2 - a{x_2}^3 + b{x_2}^2 - z_2 + I_{ext} - k\rho(\varphi_2)x_2 = 0 \\ c - d{x_2}^2 - y_2 = 0 \\ r[s(x_2 + 1.6) - z_2] = 0 \\ k_1 x_2 - k_2\varphi_2 + G_{in}(\varphi_1 + \varphi_2) = 0, \end{cases} \tag{5}$$

The Jacobian matrix of (2) is yielded as

$$J = \begin{pmatrix} J_{11} & 1 & -1 & J_{14} & 0 & 0 & 0 & 0 \\ J_{21} & -1 & 0 & 0 & 0 & 0 & 0 & 0 \\ J_{31} & 0 & J_{33} & 0 & 0 & 0 & 0 & 0 \\ J_{41} & 0 & 0 & J_{44} & 0 & 0 & 0 & J_{48} \\ 0 & 0 & 0 & 0 & J_{55} & 1 & -1 & J_{58} \\ 0 & 0 & 0 & 0 & J_{65} & -1 & 0 & 0 \\ 0 & 0 & 0 & 0 & J_{75} & 0 & J_{77} & 0 \\ 0 & 0 & 0 & J_{84} & J_{85} & 0 & 0 & J_{88} \end{pmatrix} \tag{6}$$

where $J_{11} = 2bx_1 - 3ax_1^2 - k(\alpha + 3\beta\varphi_1^2)$; $J_{21} = -2dx_1$; $J_{31} = J_{75} = rs$; $J_{85} = J_{41} = k_1$; $J_{14} = -6k\beta\varphi_1 x_1$; $J_{33} = J_{77} = -r$; $J_{44} = -k_2 - G_{in}$; $J_{48} = -G_{in}$; $J_{55} = 2bx_2 - 3ax_2^2 - k(\alpha + 3\beta\varphi_2^2)$; $J_{65} = -2dx_2$; $J_{58} = -6k\beta\varphi_2 x_2$;$J_{84} = G_{in}$; $J_{88} = -k_2 + G_{in}$.

The equilibrium point of a real number solution is first found by solving equations, then replaced into the Jacobian matrix, and the stability of the equilibrium point is determined by its eigenvalue. Table 2 summarizes the findings.

Neither excitatory magnetic field coupling nor inhibitory magnetic field coupling has an equilibrium point when $G_{ex} = 0$ or $G_{in} = 0$. The applied excitation current determines the equilibrium point in excitatory magnetic field coupling, and the excitatory magnetic field coupling intensity has a minor effect on the eigenvalue but no effect on the equilibrium point. The inhibitory magnetic field coupling intensity can affect both the equilibrium point and the eigenvalue in the inhibitory magnetic field coupling. The stability of the equilibrium point varies from unstable equilibrium point to stable equilibrium point as the magnetic field coupling strength increases.

3. Numerical results and discussion

In numerical study, this section uses the fourth order Runge-Kutta algorithm to solve the dynamic equation with transient period of 1200. Neurons in the model of the initial value are set to $(x_1, y_1, z_1, \varphi_1, x_2, y_2, z_2, \varphi_2) = (0.2, 0.5, 0.1, 0.1, 0.3, 0.8, 0.2, 0.0)$, the other parameters are chosen as a=1.0, b=3.0, c=1.0, d=5.0, r=0.006, s=4, k=1, $k_1 = 0.5$, $k_2 = 0.5$, $\alpha = 0.1$, $\beta = 0.02$. For clear illustration, the influence of applied current on the electrical activity of neurons can be illustrated by the inter spike interval (ISI) bifurcation diagram.as shown in Fig.1.

Table 2: Equilibrium points and their corresponding eigenvalues and stabilities

parameters	Remarks	Equilibrium points eigenvalues	Stabilities
$I_{ext} = 3.2$, $G_{ex} = 0.2$	Equilibrium points	-0.6865, -1.3561, 3.6542, -1.3729, -0.6865, -1.3561, 3.6542, -1.3729	Unstable saddle point
	eigenvalues	-6.8806, -6.8801, -0.8992, -0.4939, 0.1289, 0.1225, 0.0197 ,0.0213	
$I_{ext} = 3.2$, $G_{ex} = 0.8$	Equilibrium points	-0.6865, -1.3561, 3.6542, -1.3729, -0.6865, -1.3561, 3.6542, -1.3729	Unstable saddle point
	eigenvalues	-6.8806, -6.8783, -2.1052, 0.0213, -0.4939, 0.1342, 0.1225, 0.0187	
$I_{ext} = 3.2$, $G_{ex} = 2$	Equilibrium points	-0.6865, -1.3561, 3.6542, -1.3729, -0.6865, -1.3561, 3.6542, -1.3729	Unstable saddle point
	eigenvalues	-6.8806, -6.8693, -4.5161, 0.0213, -0.4939, 0.1365, 0.1225, 0.0183	
$I_{ext} = 3.2$, $G_{in} = 0.2$	Equilibrium points	-0.7000, -1.4499, 3.6001, -0.3130, -0.6587, -1.1694, 3.7652, -2.4043	Unstable saddle-focus
	eigenvalues	-6.9387, -6.7784, -0.6976±0.2024i, 0.1508, 0.0739, 0.0160, 0.0382	
$I_{ext} = 3.2$, $G_{in} = 0.8$	Equilibrium points	-0.6538, -1.1374, 3.7847, 2.5494, -0.5515, -0.5207, 4.1940, -4.9600	Unstable saddle-focus
	eigenvalues	-6.7882, -6.5947, -1.3027±0.8024i, 0.1048, 0.0259, -0.0202±0.0582i	
$I_{ext} = 3.2$, $G_{in} = 1.4$	Equilibrium points	-0.5654, -0.5986, 4.1383, 4.6618, -0.4690, -0.0997, 4.5241, -6.7307	Unstable saddle-focus
	eigenvalues	-6.6408, -6.7855, -1.9026±1.4007i, -0.1846, 0.0022±0.0597i, -0.0255	
$I_{ext} = 3.2$, $G_{in} = 1.5$	Equilibrium points	-0.5517, -0.5220, 4.1931, 4.9551, -0.4580, -0.0490, 4.5678, -6.9746	Stable focus-node
	eigenvalues	-6.6418, -6.8424, -2.0024±1.5005i, -0.2134, -0.0102±0.0601i, -0.0226	
$I_{ext} = 3.2$, $G_{in} = 2$	Equilibrium points	-0.4913, -0.2067, 4.4350, 6.2435, -0.4120, 0.1513, 4.7520, -8.0501	Stable focus-node
	eigenvalues	-6.7493, -7.1999, -2.5013±1.9992i, -0.3363, -0.1025, -0.0430, -0.0159	

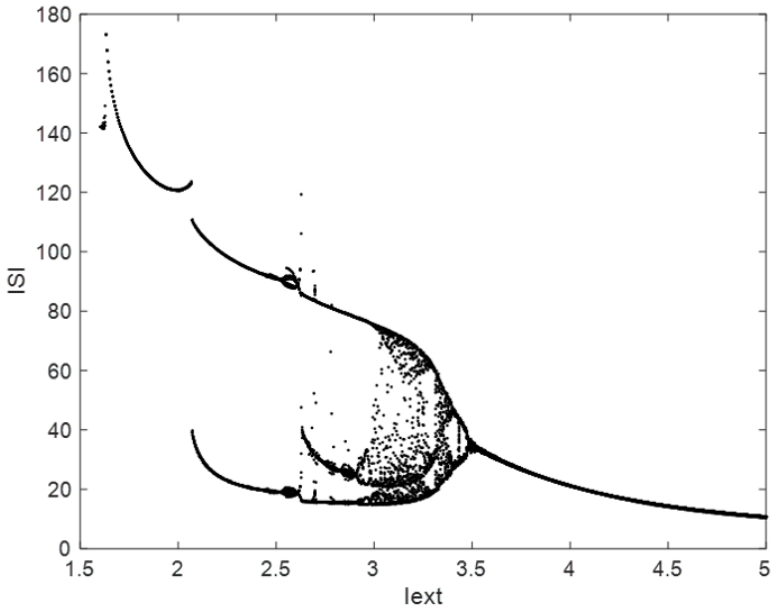

Figure 1: Bifurcation diagram of neuron membrane potential and different external stimulus signals

ISI reflects the distance between two peaks in the firing sequence diagram of neurons. It is obvious that the firing modes of HR neuronal model experienced several prominent transitions. When the external stimulus I_{ext} is too small, the neuron is in the quiescent state, and then with the increase of external stimulation, the neuron experiences spike discharge, burst discharge, chaotic discharge and periodic oscillation. We can select the appropriate external excitation current to control the firing mode of neurons, as shown in Fig. 2.

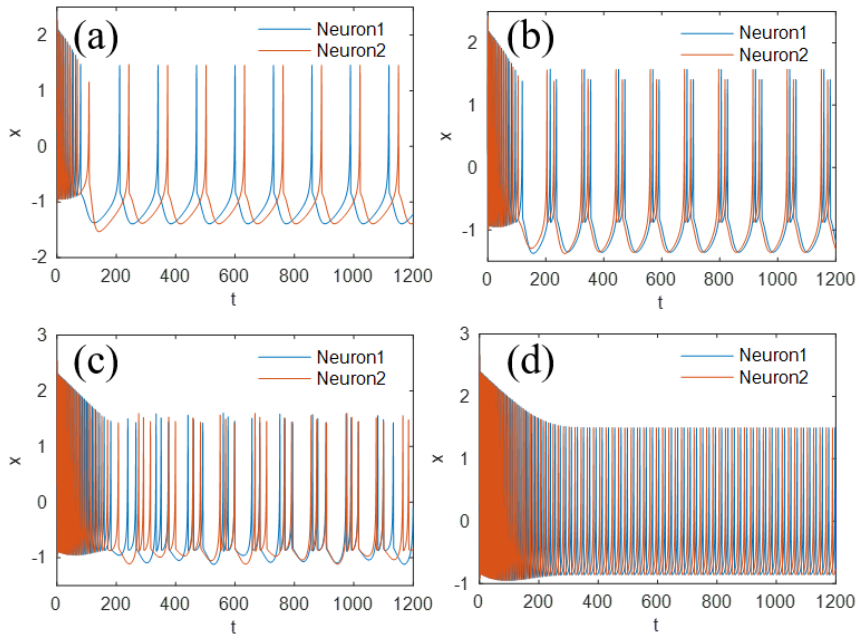

Figure 2: Two neurons with different initial values were sampled with different excitation (the blue is the response of the first neuron, and the orange is the response of the second neuron). (a) I_{ext} =1.8;(b) I_{ext} =2.3; (c) I_{ext} =3.2; (d) I_{ext} =4; The initial values are selected as (0.2, 0.5, 0.1, 0.1, 0.3, 0.8, 0.2, 0.0)

As shown in Fig. 2, various modes of electrical activity can be triggered by selecting the right applied excitation current. And two neurons with different initial values fired in the same pattern without synaptic coupling or magnetic coupling. When the external excitation current is fixed, the regulation of magnetic field coupling on neuron excitation or inhibition under different discharge modes is explored through bifurcation analysis of magnetic field coupling intensity.

3.1. Inhibitory magnetic field coupling

In case 1, two neurons with different initial values at peak discharge were selected to change the intensity of magnetic field coupling, and the effect of magnetic field coupling on neuron firing mode was detected. Bifurcation of I_{ext} with parameter G_{in} and neuron firing patterns are shown in Fig. 3 and Fig. 4.

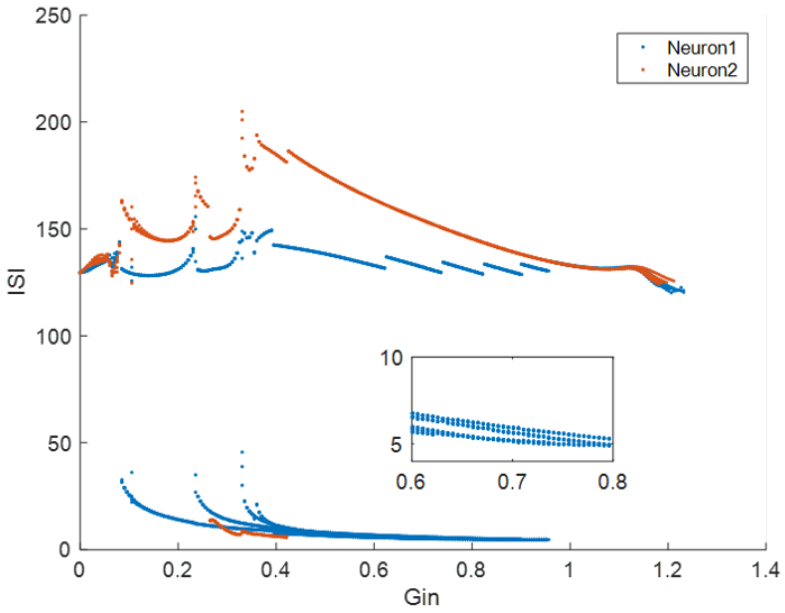

Figure 3: Bifurcation diagram of neuronal firing ISI with different Inhibitory magnetic field coupling intensity (the blue is the response of the first neuron, and the orange is the response of the second neuron)

It has been discovered that changing the magnetic coupling strength alters the firing mode of neurons. With the increase of magnetic field coupling intensity, the firing mode of neuron 1 becomes more and more complex, and the observed spikes become more and more intensive. To observe the bifurcation diagram in greater detail, zoom in on the bifurcation diagram near $G_{in} = 0.8$. Until the magnetic field coupling intensity reaches a certain degree, the neuron starts to inhibit the firing. We can find that the bifurcation diagram disappears, indicating that the neuron is stationary. With the increase of magnetic coupling intensity, the amplitude and frequency of the

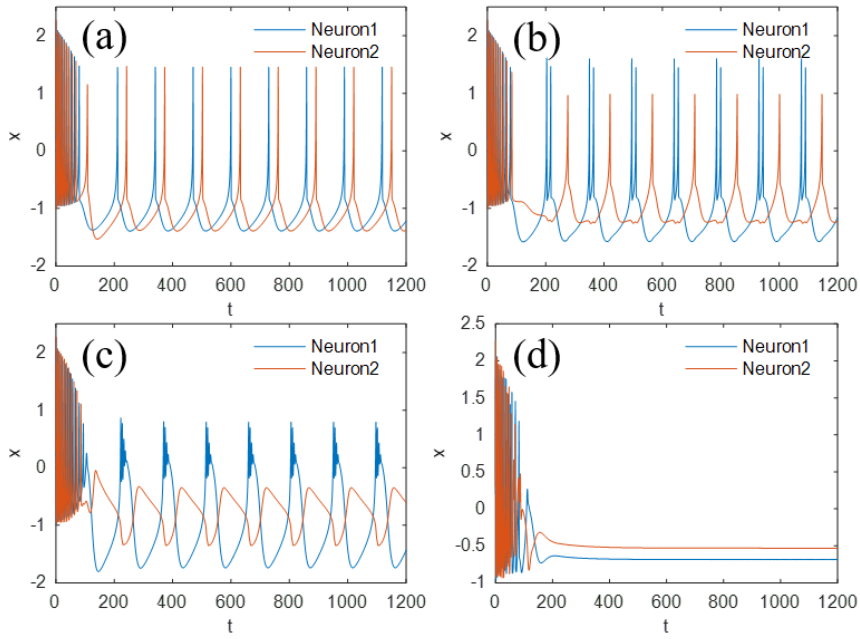

Figure 4: Two neurons with different initial values were sampled with different Inhibitory magnetic field coupling intensity (the blue is the response of the first neuron, and the orange is the response of the second neuron). (a) $G_{in} = 0$; (b) $G_{in} = 0.2$; (c)$G_{in} = 0.8$; (d) $G_{in} = 2$ The initial values are selected as (0.2, 0.5, 0.1, 0.1, 0.3, 0.8, 0.2, 0.0)

membrane potential of neuron 2 became smaller and smaller, and reached the quiescent state before neuron 1.

In case 2, the intensity of magnetic field coupling was changed to detect the influence of magnetic field coupling on neuron firing mode. The bifurcation diagram of ISI and the time series diagram are shown in Fig. 5 and Fig. 6.

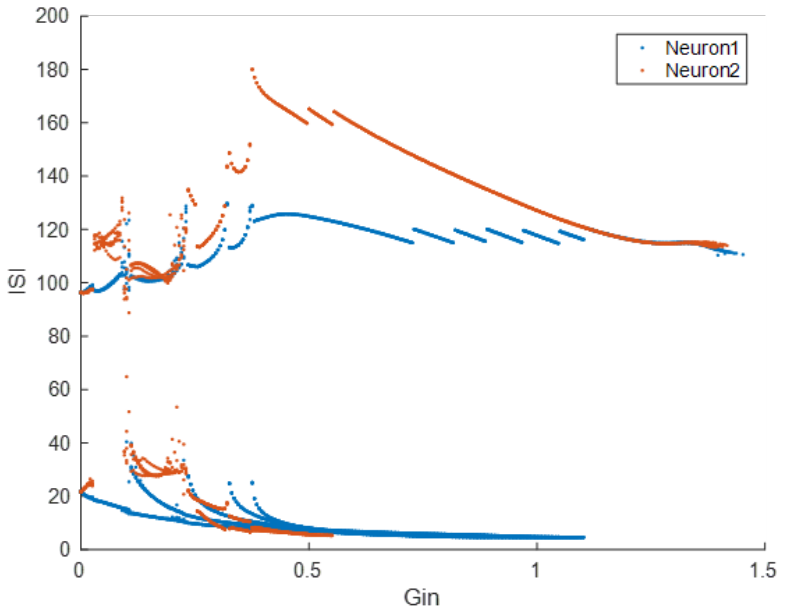

Figure 5: Bifurcation diagram of neuron with different Inhibitory magnetic field coupling intensity (the blue is the response of the first neuron, and the orange is the response of the second neuron)

With the increase of excitation current, more inhibitory magnetic field coupling is needed to make the neuron reach the quiescent state. The different discharge patterns of two neurons were observed. The two neurons move from the same firing mode to a different firing mode as a result of inhibitory magnetic coupling.Fig.6 shows the existence of burst discharge and subthreshold oscillation, and the existence of burst discharge and chaotic state. And when the neuron is stationary, the membrane potential of neuron 1 is lower than that of neuron 2.

In case 3, two neurons with different initial values at chaotic discharge were selected to change the intensity of magnetic field coupling, and the effect

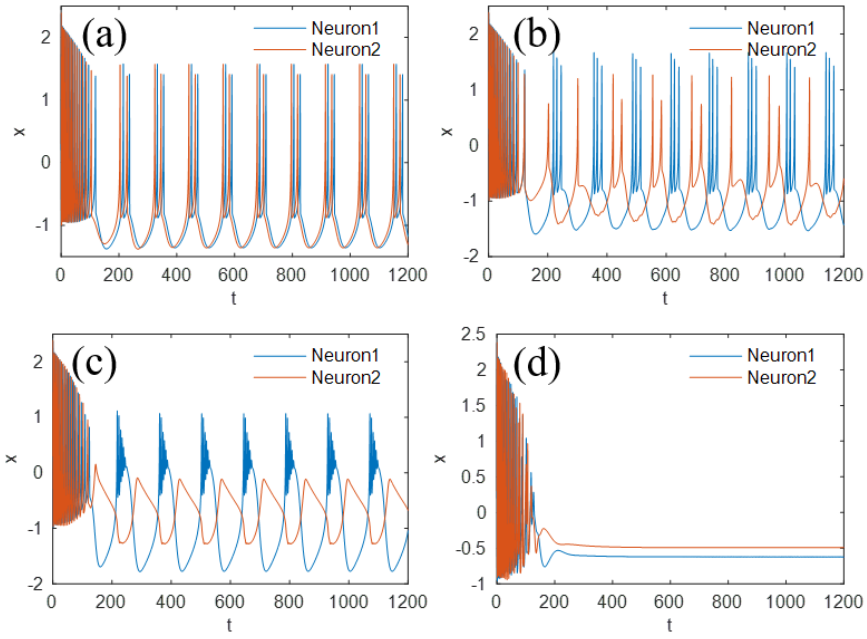

Figure 6: Two neurons with different initial values were sampled with different Inhibitory magnetic field coupling intensity (the blue is the response of the first neuron, and the orange is the response of the second neuron). (a) $G_{in} = 0$; (b) $G_{in} = 0.2$; (c)$G_{in} = 0.8$; (d) $G_{in} = 2$ The initial values are selected as (0.2, 0.5, 0.1, 0.1, 0.3, 0.8, 0.2, 0.0)

of magnetic field coupling on neuron firing mode was detected. Bifurcation of ISI with parameter Gin and neuron firing patterns are shown in Fig. 7and Fig. 8.

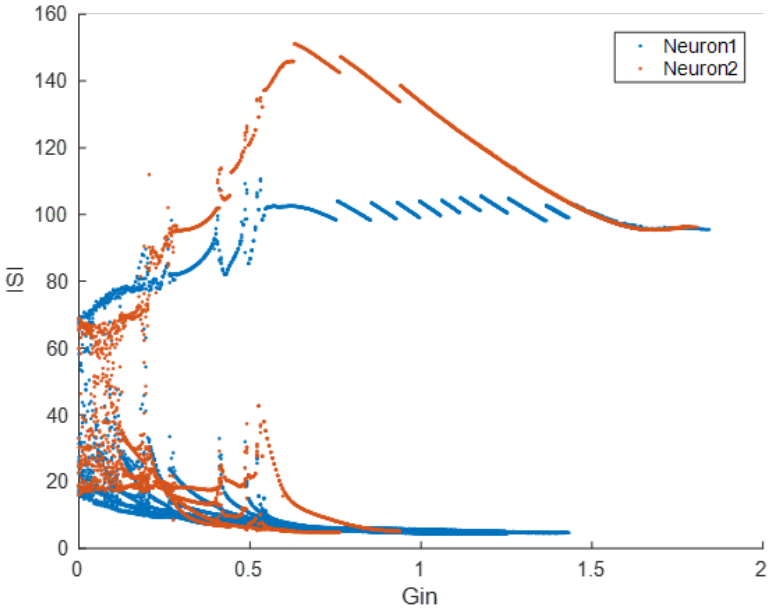

Figure 7: Bifurcation diagram of neuron with different Inhibitory magnetic field coupling intensity (the blue is the response of the first neuron, and the orange is the response of the second neuron)

As can be seen from the diagram, neurons can have a variety of discharge modes by adjusting the magnetic field coupling intensity. With the increase of magnetic field coupling intensity, the discharge modes of the two neurons change from chaos state to burst state and period-1 discharge and static state.

In case 4, two neurons at periodic oscillation were selected to change the intensity of magnetic field coupling, and the effect of magnetic field coupling on neuron firing mode was detected. Bifurcation of ISI with parameter Gin and neuron firing patterns are shown in Fig. 9 and Fig. 10.

The discharge mode can be controlled by selecting suitable magnetic coupling intensity. The two neurons move from the same firing mode to a different firing mode as a result of inhibitory magnetic coupling. When Gin=2, the neuron firing pattern is subthreshold oscillation rather than resting, as

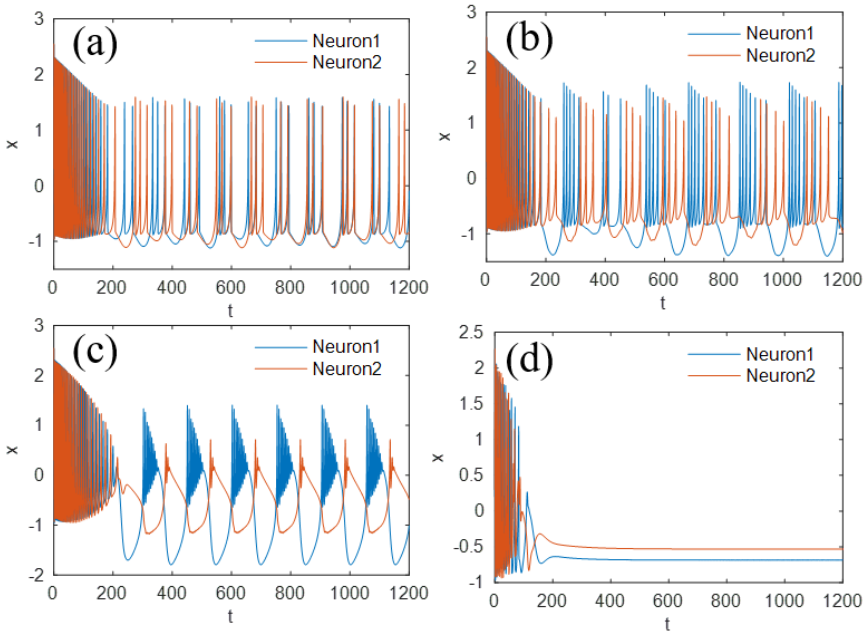

Figure 8: Two neurons with different initial values were sampled with different Inhibitory magnetic field coupling intensity (the blue is the response of the first neuron, and the orange is the response of the second neuron). (a) $G_{in} = 0$; (b) $G_{in} = 0.2$; (c)$G_{in} = 0.8$; (d) $G_{in} = 2$ The initial values are selected as (0.2, 0.5, 0.1, 0.1, 0.3, 0.8, 0.2, 0.0)

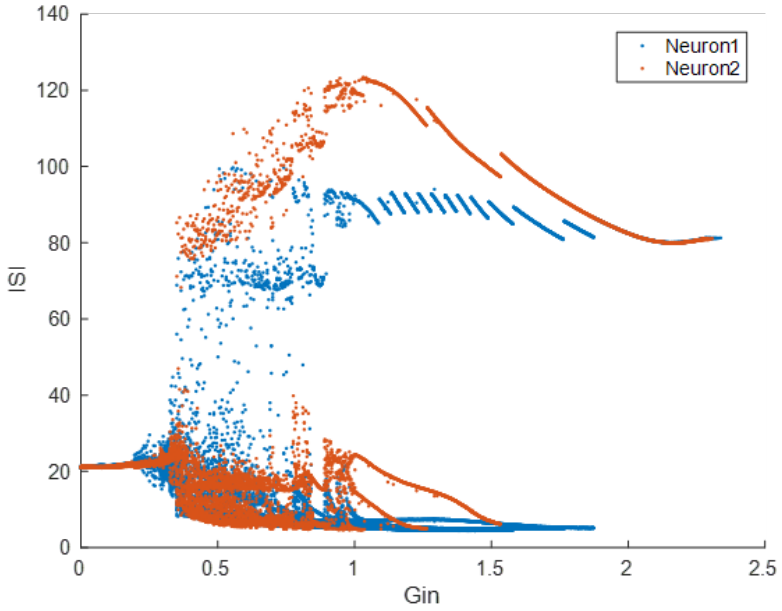

Figure 9: Bifurcation diagram of neuron with different Inhibitory magnetic field coupling intensity (the blue is the response of the first neuron, and the orange is the response of the second neuron)

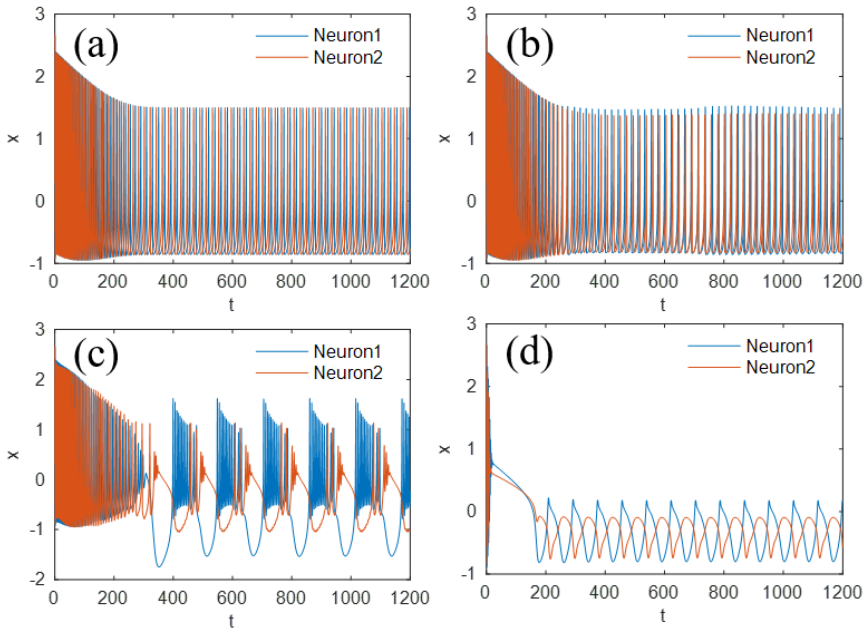

Figure 10: Two neurons with different initial values were sampled with different Inhibitory magnetic field coupling intensity (the blue is the response of the first neuron, and the orange is the response of the second neuron). (a) $G_{in} = 0$; (b) $G_{in} = 0.2$; (c)$G_{in} = 0.8$; (d) $G_{in} = 2$ The initial values are selected as (0.2, 0.5, 0.1, 0.1, 0.3, 0.8, 0.2, 0.0)

shown in Fig. 10(d). And with the increase of external stimulus current, the two neurons need more inhibitory magnetic coupling strength to reach the resting state.

3.2. Excitatory magnetic field coupling

In case 1, Two neurons with peak discharge were stimulated by an excitatory coupling magnetic field, and then the coupling intensity was changed to observe the discharge of the neurons without synaptic coupling, the results are presented in Fig.11 and Fig 12.

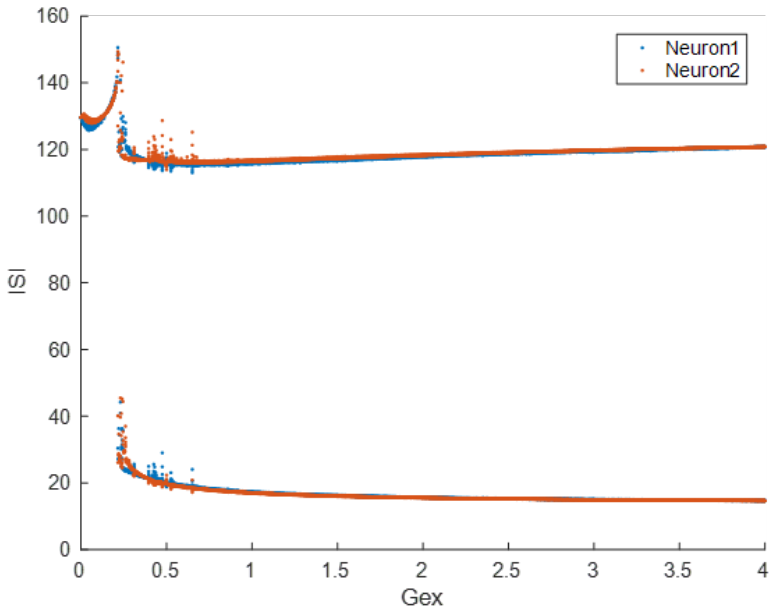

Figure 11: Bifurcation diagram of neuron with different excitatory magnetic field coupling intensity (the blue is the response of the first neuron, and the orange is the response of the second neuron)

With the increase of magnetic coupling intensity, the firing mode of the two neurons becomes more and more complex, and the observed spikes become denser. The firing mode of the neurons changes from peak discharge to period-2 discharge.

In case 2, Two neurons with burst discharge were stimulated by an excitatory coupling magnetic field, and then the coupling intensity was changed

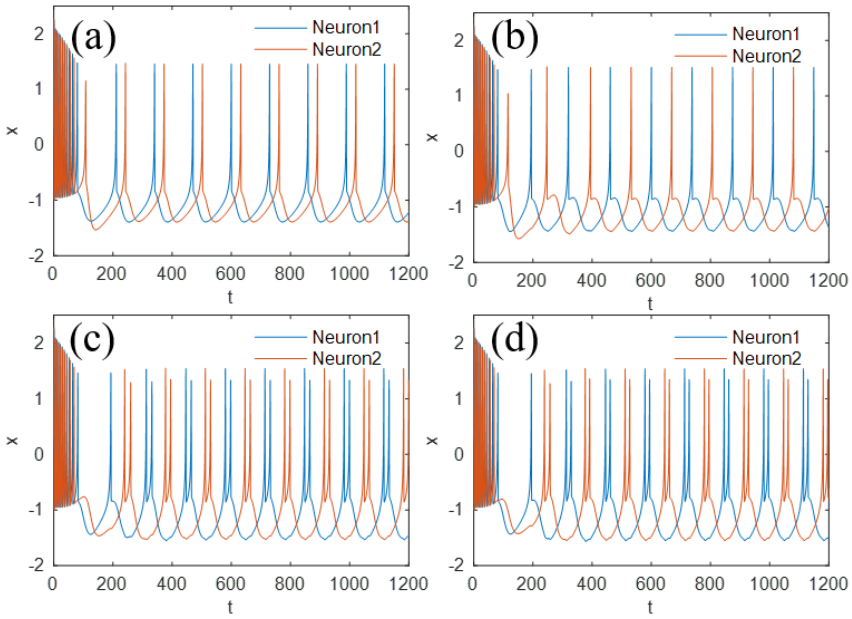

Figure 12: Two neurons with different initial values were sampled with different excitatory magnetic field coupling intensity (the blue is the response of the first neuron, and the orange is the response of the second neuron). (a) $G_{ex} = 0$; (b) $G_{ex} = 0.2$; (c)$G_{ex} = 0.8$; (d) $G_{ex} = 2$ The initial values are selected as (0.2, 0.5, 0.1, 0.1, 0.3, 0.8, 0.2, 0.0)

to observe the discharge of the neurons without synaptic coupling, the results are presented in Fig. 13 and Fig. 14.

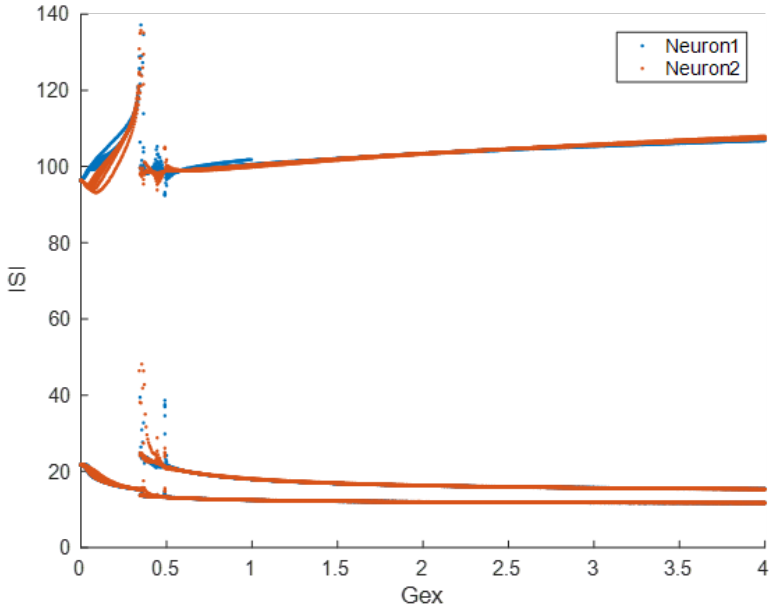

Figure 13: Bifurcation diagram of neuron with different excitatory magnetic field coupling intensity (the blue is the response of the first neuron, and the orange is the response of the second neuron)

Neurons firing in period-2 discharge flip to firing in period-3 discharge after being activated by an excitatory magnetic coupling. And it was found that excitatory magnetic fields made neurons asynchronous.

In case 3, Two neurons with chaotic discharge were stimulated by an excitatory coupling magnetic field, and then the coupling intensity was changed to observe the discharge of the neurons without synaptic coupling, the results are presented in Fig.15 and Fig. 16.

The bifurcation diagram shows that the two neurons are in chaotic discharge, but through the sequence diagram, we can find that the excitatory magnetic coupling promotes the neuron discharge.

In case 4, Two neurons with Periodic oscillation were stimulated by an excitatory coupling magnetic field, and then the coupling intensity was changed to observe the discharge of the neurons without synaptic coupling, the results are presented in Fig.17 and Fig. 18.

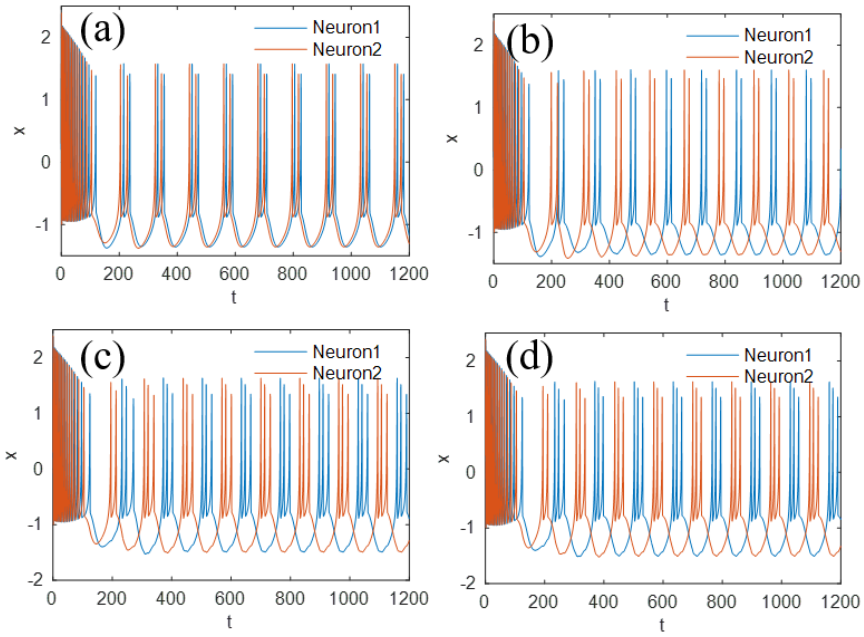

Figure 14: Two neurons with different initial values were sampled with different excitatory magnetic field coupling intensity (the blue is the response of the first neuron, and the orange is the response of the second neuron). (a) $G_{ex} = 0$; (b) $G_{ex} = 0.2$; (c)$G_{ex} = 0.8$; (d) $G_{ex} = 2$ The initial values are selected as (0.2, 0.5, 0.1, 0.1, 0.3, 0.8, 0.2, 0.0)

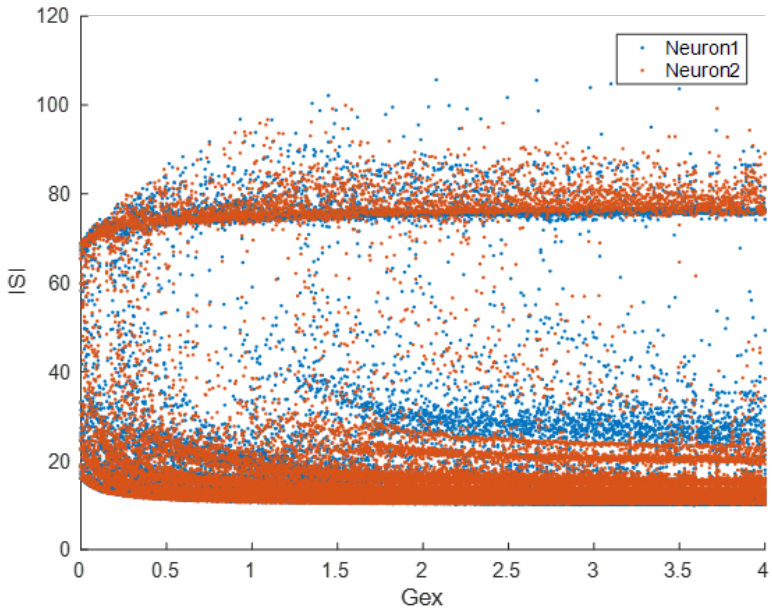

Figure 15: Bifurcation diagram of neuron with different excitatory magnetic field coupling intensity (the blue is the response of the first neuron, and the orange is the response of the second neuron)

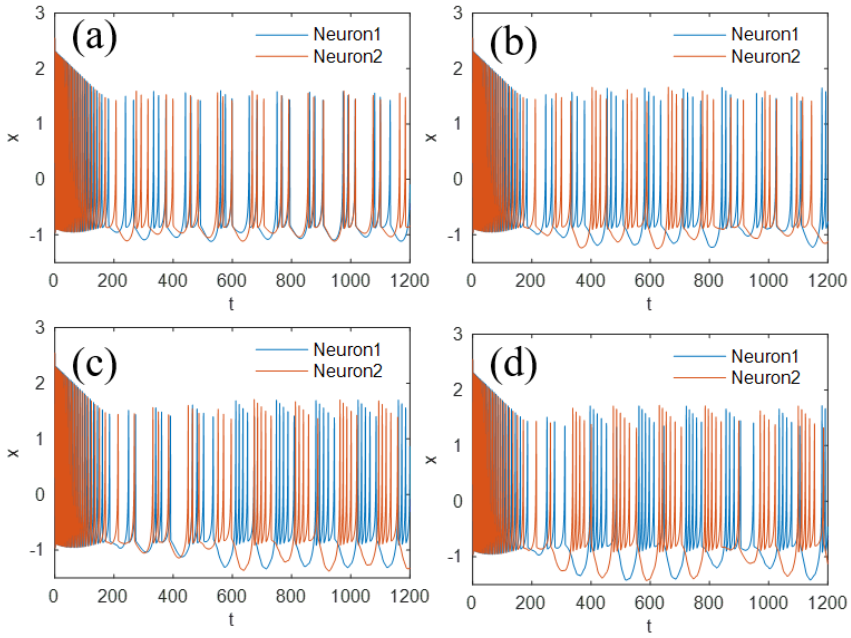

Figure 16: Two neurons with different initial values were sampled with different excitatory magnetic field coupling intensity (the blue is the response of the first neuron, and the orange is the response of the second neuron). (a) $G_{ex} = 0$; (b) $G_{ex} = 0.2$; (c)$G_{ex} = 0.8$; (d) $G_{ex} = 2$ The initial values are selected as (0.2, 0.5, 0.1, 0.1, 0.3, 0.8, 0.2, 0.0)

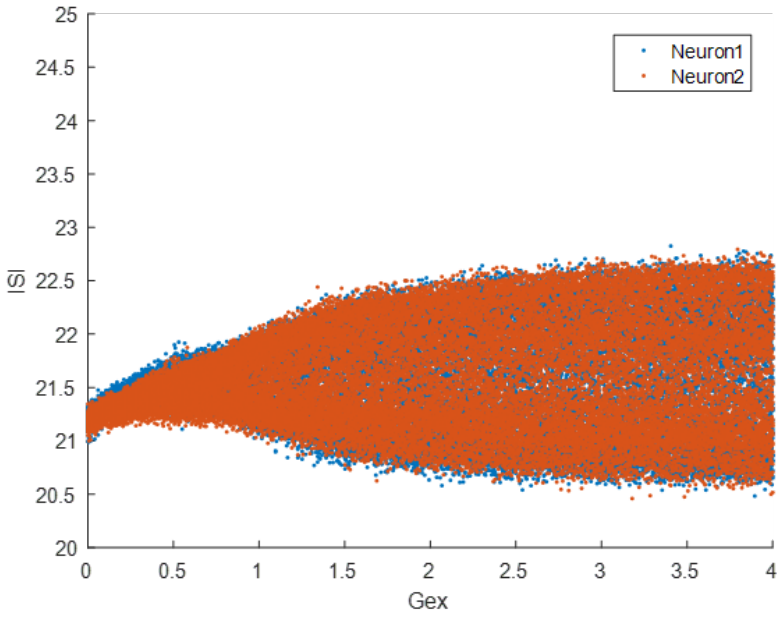

Figure 17: Bifurcation diagram of neuron with different excitatory magnetic field coupling intensity (the blue is the response of the first neuron, and the orange is the response of the second neuron)

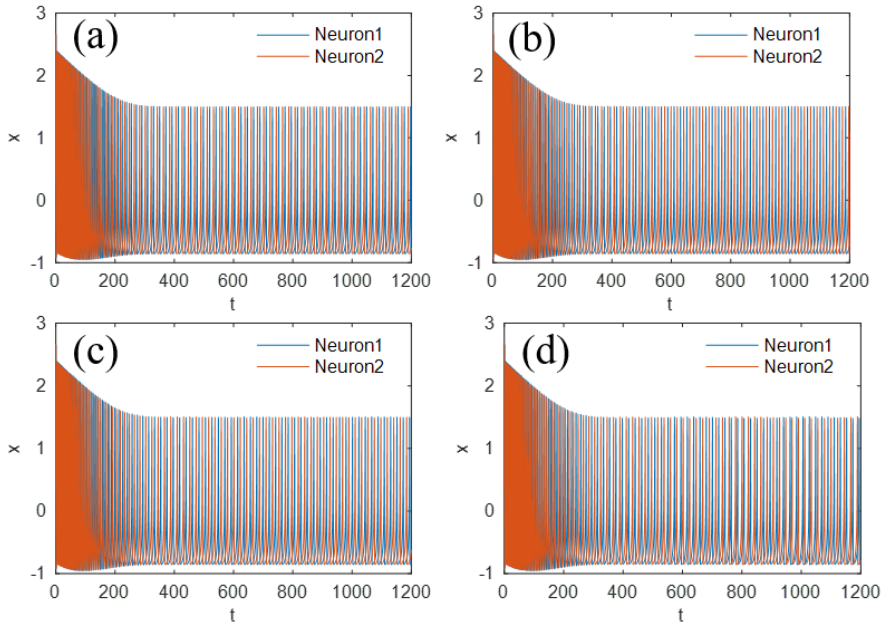

Figure 18: Two neurons with different initial values were sampled with different excitatory magnetic field coupling intensity (the blue is the response of the first neuron, and the orange is the response of the second neuron). (a) $G_{ex} = 0$; (b) $G_{ex} = 0.2$; (c)$G_{ex} = 0.8$; (d) $G_{ex} = 2$ The initial values are selected as (0.2, 0.5, 0.1, 0.1, 0.3, 0.8, 0.2, 0.0)

In conclusion, magnetic coupling has the ability to impact neuronal excitement or inhibition. Excitatory magnetic field coupling can benefit to neuron firing, but it can also affect neuron firing patterns, complicate electrical activity. Inhibitory magnetic field coupling can enhance neuron firing when the coupling intensity is small, but it can inhibit neuron firing when the coupling intensity is strong. The neurons enter a static state when the magnetic coupling strength reaches a critical point. As the external stimulus current increases, more inhibitory magnetic field coupling strength is required to make the neuron enter the quiescent state.

4. Conclusions

Table 3 lists the synaptic coupling and magnetic coupling models of neurons. In contrast to electrical synapses, magnetic coupling has inhibitory effects. Chemical synaptic coupling is unidirectional, while magnetic coupling is bidirectional and has no time delay. As a means of information transmission between neurons, magnetic field coupling may have similar properties to synaptic coupling. In this paper, we explore the modulation of neural excitation and inhibition by magnetic coupling. The electrical activity of neurons can be promoted by increasing the magnetic coupling intensity of the excitatory model. A high enough inhibitory magnetic coupling intensity to make the neuron quiescent. These results have a certain significance for further revealing the mechanism of information interaction between neurons.

5. Acknowledgement

This work is supported by the Major Research Plan of the National Natural Science Foundation of China (No.61971185), the National Natural Science Foundation of China (No.91964108) and Natural Science Foundation of Hunan Province(2020JJ4218).

6. Declaration of Competing Interest

The authors declare that they have no known competing financial interests or personal relationships that could have appeared to influence the work in this paper.

Table 3: Different ways of coupling HR neurons

Different coupling	Equations	Remarks
Excitatory electrical synaptic coupling	$\begin{cases} \dot{x}_1 = y_1 - a{x_1}^3 + b{x_1}^2 - z_1 + I_{ext} - k\rho(\varphi)x_1 + D(x_2 - x_1) \\ \dot{y}_1 = c - d{x_1}^2 - y_2 \\ \dot{z}_1 = r[s(x_1 + 1.6) - z_1] \\ \dot{\varphi}_1 = k_1 x_1 - k_2\varphi_1 \\ \dot{x}_2 = y_2 - a{x_2}^3 + b{x_2}^2 - z_2 + I_{ext} - k\rho(\varphi)x_2 + D(x_1 - x_2) \\ \dot{y}_2 = c - d{x_2}^2 - y_2 \\ \dot{z}_2 = r[s(x_2 + 1.6) - z_2] \\ \dot{\varphi}_2 = k_1 x_2 - k_2\varphi_2, \end{cases}$	bidirectional coupling, electric field
Excitatory chemical synaptic coupling	$\begin{cases} \dot{x}_1 = y_1 - a{x_1}^3 + b{x_1}^2 - z_1 + I_{ext} - k\rho(\varphi)x_1 \\ \dot{y}_1 = c - d{x_1}^2 - y_2 \\ \dot{z}_1 = r[s(x_1 + 1.6) - z_1] \\ \dot{\varphi}_1 = k_1 x_1 - k_2\varphi_1 \\ \dot{x}_2 = y_2 - a{x_2}^3 + b{x_2}^2 - z_2 + I_{ext} - k\rho(\varphi)x_2 \\ +g_{ex}(v_{se} - x_2)(\frac{1}{1+e^{(-\lambda(x_1(t-\tau_c)-\theta))}}) \qquad v_{se} > x_{2\max} \\ \dot{y}_2 = c - d{x_2}^2 - y_2 \\ \dot{z}_2 = r[s(x_2 + 1.6) - z_2] \\ \dot{\varphi}_2 = k_1 x_2 - k_2\varphi_2, \end{cases}$	unidirectional coupling, time delay, neurotransmitter
Inhibitory chemical synaptic coupling	$\begin{cases} \dot{x}_1 = y_1 - a{x_1}^3 + b{x_1}^2 - z_1 + I_{ext} - k\rho(\varphi)x_1 \\ \dot{y}_1 = c - d{x_1}^2 - y_2 \\ \dot{z}_1 = r[s(x_1 + 1.6) - z_1] \\ \dot{\varphi}_1 = k_1 x_1 - k_2\varphi_1 \\ \dot{x}_2 = y_2 - a{x_2}^3 + b{x_2}^2 - z_2 + I_{ext} - k\rho(\varphi)x_2 \\ +g_{in}(v_{se} - x_2)(\frac{1}{1+e^{(-\lambda(x_1(t-\tau_c)-\theta))}}) \qquad v_{se} < x_{2\min} \\ \dot{y}_2 = c - d{x_2}^2 - y_2 \\ \dot{z}_2 = r[s(x_2 + 1.6) - z_2] \\ \dot{\varphi}_2 = k_1 x_2 - k_2\varphi_2, \end{cases}$	unidirectional coupling, time delay, neurotransmitter
Excitatory magnetic field coupling	$\begin{cases} \dot{x}_1 = y_1 - a{x_1}^3 + b{x_1}^2 - z_1 + I_{ext} - k\rho(\varphi)x_1 \\ \dot{y}_1 = c - d{x_1}^2 - y_2 \\ \dot{z}_1 = r[s(x_1 + 1.6) - z_1] \\ \dot{\varphi}_1 = k_1 x_1 - k_2\varphi_1 + G_{ex}(\varphi_2 - \varphi_1) \\ \dot{x}_2 = y_2 - a{x_2}^3 + b{x_2}^2 - z_2 + I_{ext} - k\rho(\varphi)x_2 \\ \dot{y}_2 = c - d{x_2}^2 - y_2 \\ \dot{z}_2 = r[s(x_2 + 1.6) - z_2] \\ \dot{\varphi}_2 = k_1 x_2 - k_2\varphi_2 + G_{ex}(\varphi_1 - \varphi_2), \end{cases}$	bidirectional coupling, magnetic field
Inhibitory magnetic field coupling	$\begin{cases} \dot{x}_1 = y_1 - a{x_1}^3 + b{x_1}^2 - z_1 + I_{ext} - k\rho(\varphi)x_1 \\ \dot{y}_1 = c - d{x_1}^2 - y_2 \\ \dot{z}_1 = r[s(x_1 + 1.6) - z_1] \\ \dot{\varphi}_1 = k_1 x_1 - k_2\varphi_1 - G_{in}(\varphi_2 + \varphi_1) \\ \dot{x}_2 = y_2 - a{x_2}^3 + b{x_2}^2 - z_2 + I_{ext} - k\rho(\varphi)x_2 \\ \dot{y}_2 = c - d{x_2}^2 - y_2 \\ \dot{z}_2 = r[s(x_2 + 1.6) - z_2] \\ \dot{\varphi}_2 = k_1 x_2 - k_2\varphi_2 + G_{in}(\varphi_1 + \varphi_2), \end{cases}$	bidirectional coupling, magnetic field

References

[1] L. Chua, Memristor-the missing circuit element, IEEE Transactions on Circuit Theory 18 (5) (1971) 507–519. doi:10.1109/TCT.1971.1083337.

[2] H. Chang, Q. Song, Y. Li, Z. Wang, G. Chen, Unstable limit cycles and singular attractors in a two-dimensional memristor-based dynamic system, Entropy 21 (4) (2019). doi:10.3390/e21040415.

[3] X. Ma, J. Mou, L. Xiong, S. Banerjee, Y. Cao, J. Wang, A novel chaotic circuit with coexistence of multiple attractors and state transition based on two memristors, Chaos, Solitons Fractals 152 (2021) 111363. doi:https://doi.org/10.1016/j.chaos.2021.111363.

[4] X. Zhang, Z. Tian, J. Li, Z. Cui, A simple parallel chaotic circuit based on memristor, Entropy 23 (6) (2021). doi:10.3390/e23060719.

[5] S. Zhang, J. Zheng, X. Wang, Z. Zeng, A novel no-equilibrium hr neuron model with hidden homogeneous extreme multistability, Chaos, Solitons Fractals 145 (2021) 110761. doi:https://doi.org/10.1016/j.chaos.2021.110761.

[6] V. Varshney, S. Sabarathinam, A. Prasad, K. Thamilmaran, Infinite number of hidden attractors in memristor-based autonomous duffing oscillator, International Journal of Bifurcation and Chaos 28 (01) (2018) 1850013. doi:10.1142/S021812741850013X.

[7] Q. Deng, C. Wang, L. Yang, Four-wing hidden attractors with one stable equilibrium point, International Journal of Bifurcation and Chaos 30 (06) (2020) 2050086. doi:10.1142/S0218127420500868.

[8] X. Min, X. Wang, P. Zhou, S. Yu, H. H.-C. Iu, An optimized memristor-based hyperchaotic system with controlled hidden attractors, IEEE Access 7 (2019) 124641–124646. doi:10.1109/ACCESS.2019.2938183.

[9] H. Wu, Y. Ye, B. Bao, M. Chen, Q. Xu, Memristor initial boosting behaviors in a two-memristor-based hyperchaotic system, Chaos, Solitons Fractals 121 (2019) 178–185. doi:https://doi.org/10.1016/j.chaos.2019.03.005.

[10] F. Yu, L. Liu, H. Shen, Z. Zhang, Y. Huang, C. Shi, S. Cai, X. Wu, S. Du, Q. Wan, Dynamic analysis, circuit design, and synchronization of a novel 6d memristive four-wing hyperchaotic system with multiple coexisting attractors, Complexity 2020 (2020). doi:10.1155/2020/5904607.

[11] D. Yan, L. Wang, S. Duan, J. Chen, J. Chen, Chaotic attractors generated by a memristor-based chaotic system and julia fractal, Chaos, Solitons Fractals 146 (2021) 110773. doi:https://doi.org/10.1016/j.chaos.2021.110773.

[12] H. Lin, C. Wang, F. Yu, C. Xu, Q. Hong, W. Yao, Y. Sun, An extremely simple multiwing chaotic system: Dynamics analysis, encryption application, and hardware implementation, IEEE Transactions on Industrial Electronics 68 (12) (2021) 12708–12719. doi:10.1109/TIE.2020.3047012.

[13] Y. Hu, Q. Li, D. Ding, L. Jiang, Z. Yang, H. Zhang, Z. Zhang, Multiple coexisting analysis of a fractional-order coupled memristive system and its application in image encryption, Chaos, Solitons Fractals 152 (2021) 111334. doi:https://doi.org/10.1016/j.chaos.2021.111334.

[14] Y. Yang, L. Wang, S. Duan, L. Luo, Dynamical analysis and image encryption application of a novel memristive hyperchaotic system, Optics Laser Technology 133 (2021) 106553. doi:https://doi.org/10.1016/j.optlastec.2020.106553.

[15] H. Lin, C. Wang, C. Chen, Y. Sun, C. Zhou, C. Xu, Q. Hong, Neural bursting and synchronization emulated by neural networks and circuits, IEEE Transactions on Circuits and Systems I: Regular Papers 68 (8) (2021) 3397–3410. doi:10.1109/TCSI.2021.3081150.

[16] C. Xu, C. Wang, J. Jiang, J. Sun, H. Lin, Memristive circuit implementation of context-dependent emotional learning network and its application in multi-task, IEEE Transactions on Computer-Aided Design of Integrated Circuits and Systems (2021) 1–1doi:10.1109/TCAD.2021.3116463.

[17] L. Yang, C. Wang, Emotion model of associative memory possessing variable learning rates with time delay, Neurocomputing 460 (2021) 117–125. doi:https://doi.org/10.1016/j.neucom.2021.07.011.

[18] W. Xie, C. Wang, H. Lin, A fractional-order multistable locally active memristor and its chaotic system with transient transition, state jump, Nonlinear Dynamics 104 (4) (2021) 4523–4541. doi:10.1007/s11071-021-06476-2.

[19] J. Chen, C. Li, T. Huang, X. Yang, Global stabilization of memristor-based fractional-order neural networks with delay via output-feedback control, Modern Physics Letters B 31 (05) (2017) 1750031. doi:10.1142/S0217984917500312.

[20] H. Jahanshahi, A. Yousefpour, J. M. Munoz-Pacheco, S. Kacar, V.-T. Pham, F. E. Alsaadi, A new fractional-order hyperchaotic memristor oscillator: Dynamic analysis, robust adaptive synchronization, and its application to voice encryption, Applied Mathematics and Computation 383 (2020) 125310. doi:https://doi.org/10.1016/j.amc.2020.125310.

[21] H. Lin, C. Wang, Y. Sun, W. Yao, Firing multistability in a locally active memristive neuron model, Nonlinear Dynamics 100 (4) (2020) 3667–3683. doi:10.1007/s11071-020-05687-3.

[22] C. Li, H. Li, W. Xie, J. Du, A s-type bistable locally active memristor model and its analog implementation in an oscillator circuit, Nonlinear Dynamics 106 (1) (2021) 1041–1058. doi:10.1007/s11071-021-06814-4.

[23] Y. Dong, G. Wang, H. H.-C. Iu, G. Chen, L. Chen, Coexisting hidden and self-excited attractors in a locally active memristor-based circuit, Chaos: An Interdisciplinary Journal of Nonlinear Science 30 (10) (2020) 103123. doi:10.1063/5.0002061.

[24] M. Lv, C. Wang, G. Ren, J. Ma, X. Song, Model of electrical activity in a neuron under magnetic flow effect, Nonlinear Dynamics 85 (3) (2016) 1479–1490. doi:10.1007/s11071-016-2773-6.

[25] M. Lv, J. Ma, Multiple modes of electrical activities in a new neuron model under electromagnetic radiation, Neurocomputing 205 (2016) 375–381. doi:10.1016/j.neucom.2016.05.004.

[26] H. Bao, W. Liu, M. Chen, Hidden extreme multistability and dimensionality reduction analysis for an improved non-autonomous memristive

fitzhugh–nagumo circuit, Nonlinear Dynamics 96 (3) (2019) 1879–1894. doi:10.1007/s11071-019-04890-1.

[27] H. Bao, A. Hu, W. Liu, B. Bao, Hidden bursting firings and bifurcation mechanisms in memristive neuron model with threshold electromagnetic induction, IEEE Transactions on Neural Networks and Learning Systems 31 (2) (2019) 502–511. doi:10.1109/TNNLS.2019.2905137.

[28] J. Ma, G. Zhang, T. Hayat, G. Ren, Model electrical activity of neuron under electric field, Nonlinear dynamics 95 (2) (2019) 1585–1598. doi:10.1007/s11071-018-4646-7.

[29] B. Yan, S. Panahi, S. He, S. Jafari, Further dynamical analysis of modified fitzhugh–nagumo model under the electric field, Nonlinear Dynamics 101 (1) (2020) 521–529. doi:10.1007/s11071-020-05816-y.

[30] F. Wu, J. Ma, G. Zhang, A new neuron model under electromagnetic field, Applied Mathematics and Computation 347 (2019) 590–599. doi:10.1016/j.amc.2018.10.087.

[31] L. Lu, Y. Jia, Y. Xu, M. Ge, L. Yang, X. Zhan, Energy dependence on modes of electric activities of neuron driven by different external mixed signals under electromagnetic induction, Science China Technological Sciences 62 (3) (2019) 427–440. doi:10.1007/s11431-017-9217-x.

[32] J. Hindmarsh, R. Rose, A model of the nerve impulse using two first-order differential equations, Nature 296 (5853) (1982) 162–164. doi:10.1038/296162a0.

[33] G. Wang, Y. Xu, M. Ge, L. Lu, Y. Jia, Mode transition and energy dependence of fitzhugh-nagumo neural model driven by high-low frequency electromagnetic radiation, AEU-International Journal of Electronics and Communications 120 (2020) 153209. doi:10.1016/j.aeue.2020.153209.

[34] R. FitzHugh, Impulses and physiological states in theoretical models of nerve membrane, Biophysical journal 1 (6) (1961) 445–466. doi:10.1016/S0006-3495(61)86902-6.

[35] Y. Yang, J. Ma, Y. Xu, Y. Jia, Energy dependence on discharge mode of izhikevich neuron driven by external stimulus under electromagnetic

induction, Cognitive Neurodynamics 15 (2) (2021) 265–277. doi:10.1007/s11571-020-09596-4.

[36] E. Izhikevich, Simple model of spiking neurons, IEEE Transactions on Neural Networks 14 (6) (2003) 1569–1572. doi:10.1109/TNN.2003.820440.

[37] X. Hu, C. Liu, L. Liu, J. Ni, Y. Yao, Chaotic dynamics in a neural network under electromagnetic radiation, Nonlinear Dynamics 91 (3) (2018) 1541–1554. doi:10.1007/s11071-017-3963-6.

[38] H. Lin, C. Wang, Influences of electromagnetic radiation distribution on chaotic dynamics of a neural network, Applied Mathematics and Computation 369 (2020) 124840. doi:https://doi.org/10.1016/j.amc.2019.124840.

[39] H. Lin, C. Wang, W. Yao, Y. Tan, Chaotic dynamics in a neural network with different types of external stimuli, Communications in Nonlinear Science and Numerical Simulation 90 (2020) 105390. doi:https://doi.org/10.1016/j.cnsns.2020.105390.

[40] L. Qu, L. Du, H. Hu, Z. Cao, Z. Deng, Pattern control of external electromagnetic stimulation to neuronal networks, Nonlinear Dynamics 102 (4) (2020) 2739–2757. doi:10.1007/s11071-020-06076-6.

[41] J. Ma, L. Mi, P. Zhou, Y. Xu, T. Hayat, Phase synchronization between two neurons induced by coupling of electromagnetic field, Applied Mathematics and Computation 307 (2017) 321–328. doi:https://doi.org/10.1016/j.amc.2017.03.002.

[42] S. Guo, Y. Xu, C. Wang, W. Jin, A. Hobiny, J. Ma, Collective response, synapse coupling and field coupling in neuronal network, Chaos, Solitons Fractals 105 (2017) 120–127. doi:https://doi.org/10.1016/j.chaos.2017.10.019.

[43] Y. Zhao, X. Sun, Y. Liu, J. Kurths, Phase synchronization dynamics of coupled neurons with coupling phase in the electromagnetic field, Nonlinear Dynamics 93 (3) (2018) 1315–1324. doi:10.1007/s11071-018-4261-7.

[44] Q. Zhou, D. Q. Wei, Collective dynamics of neuronal network under synapse and field coupling, Nonlinear Dynamics 105 (1) (2021) 753–765. doi:10.1007/s11071-021-06575-0.

[45] Y. Xu, Y. Jia, J. Ma, T. Hayat, A. Alsaedi, Collective responses in electrical activities of neurons under field coupling, Scientific reports 8 (1) (2018) 1–10. doi:10.1038/s41598-018-19858-1.